

ANALYSIS OF 3D CARDIAC DEFORMATIONS WITH 3D SINMOD

Hui Wang¹, Christian T. Stoeck², Sebastian Kozerke^{2,3}, and Amir A. Amini⁴

¹MR Clinical Science, Philips Healthcare, Cleveland, OH, USA

²Institute for Biomedical Engineering, ETH Zurich, Switzerland

³Imaging Sciences and biomedical Engineering, King's College London, United Kingdom

⁴University of Louisville, Louisville, KY, USA

ABSTRACT

In this paper, we propose a novel 3D sine wave modeling (3D SinMod) approach to automatic analysis of 3D cardiac deformations. An accelerated 3D complementary spatial modulation of magnetization (CSPAMM) tagging technique was used to modulate the myocardial tissue and to acquire 3D MR data sets of the whole-heart including three orthogonal tags within three breath-holds. Each tag set is able to assess the motion along a direction perpendicular to the tag lines. With the application of CSPAMM, the effect of tag fading encountered in SPAMM tagging due to T_1 relaxation is mitigated and tag deformations can be visualized for the entire cardiac cycle, including diastolic phases. In the proposed approach, the environment around each voxel in the 3D volume is modeled as a moving sine wavefront with local frequency and amplitude. The biggest advantage of the proposed technique is that the entire framework, from data acquisition to data analysis is in the 3D domain, which permits quantification of both the in-plane and through-plane motion components. The accuracy and the effectiveness of the proposed method has been validated using both simulated and in vivo tag data.

Index Terms—MRI Tagging, 3D SinMod, Cardiac Deformations, 3D CSPAMM

I. INTRODUCTION

Since the introduction of MRI tagging technique [1], [2], many methods have been developed to detect tag features and to track the heart motion. Among these, phase-based techniques have emerged as a more commonly used method, due to their fast processing speed and reduced user interaction [3], [4], [5], [6]. It has been shown that sine wave modeling (SinMod) performs better with respect to accuracy of displacement detection and avoidance of artifacts [3]. Review articles on existing techniques can be found in references [7], [8], [9].

Most of the current techniques are applicable to 2D+t tagged MR image sequences. However, heart deforms in a 3D+t space with complex twisting motion combined with longitudinal shortening and wall thickening. 2D cardiac

motion analysis approaches often suffer from dealing with through-plane motion. 3D whole heart acquisition and image analysis have the ability of taking into account all the components of the cardiac motion. In this paper, a fully 3D complementary spatial modulation of magnetization (CSPAMM) acquisition [10] was employed. Three tagged volume series with mutually perpendicular tag lines were acquired. A novel 3D sinMod technique was then used to extract the cardiac deformation from a full 3D acquisition. SinMod is a frequency-based method for analysis of the heart displacement and deformation from tagged MRI sequences using phase information [3]. In 3D SinMod, the intensity distribution around each pixel is modeled as a cosine wave front. The principle behind 3D SinMod tracking is that both phase and frequency for each voxel are determined directly from the frequency analysis and the displacement is calculated from the quotient of phase difference and local frequency. Experiments were carried out on real image data, and on simulated data for which the ground truth is known. Qualitative and quantitative evaluations showed the reliability of the displacement fields.

The rest of this paper is organized as follows. In the following section, the data acquisition used in the experiments is presented. In section III, the 3D SinMod technique is described. In section IV, experimental results using both simulated and in-vivo human tagged MRI data are presented. Finally, conclusions are given in section V.

II. DATA ACQUISITION

The data were acquired using the 3D CSPAMM tagging sequence [10]. In three breath-holds each with 18 heartbeats, the sequence was applied three times where in each case, the tagging gradient was rotated in such a way to acquire 3D+t data with orthogonal tags. Typical imaging parameters were: FOV = $108 \times 108 \times 108 \text{ mm}^3$, matrix size = 28 (Frequency Encoding) \times 14 (Phase Encoding) \times 16 (16 in slice select direction, but only 14 out of 16 were used in reconstruction). In the spatial domain, the image matrix size was 112×112 , slice thickness = 8 mm , and tag spacing was 7 mm . Each data set consisted of 20 frames per cardiac cycle. Figure 1 shows some example mid-ventricular slices for three data

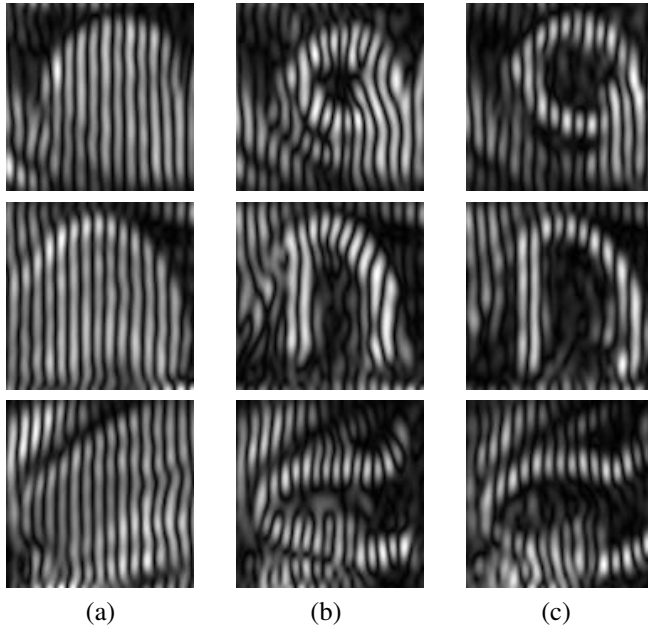


Fig. 1. Example mid-ventricular slices for three data sets (row one to row three) with orthogonal tagging directions from 3D CSPAMM sequence. (a) The first phase (at end-diastole). (b) the 10th phase (at end-systole). (c) the 20th phase (at end-diastole).

sets with orthogonal tagging directions. In this paper, we report on results of the new deformation analysis approach on 5 in-vivo human data sets.

III. METHOD

A 2D sine wave modeling (SinMod) method was previously proposed by Arts *et al.* to analyze heart displacement and deformation from 2D short axis tagged MRI data [3]. In 2D SinMod, the intensity distribution around each pixel at location (p, q) in two images is modeled as a cosine wave front:

$$\begin{aligned} I_1(p, q) &= A_1 \cos(\omega_p(p + \frac{u}{2}) + \varphi) + n_1(p, q) \\ I_2(p, q) &= A_2 \cos(\omega_p(p - \frac{u}{2}) + \varphi) + n_2(p, q) \end{aligned} \quad (1)$$

where ω_p and φ are the spatial frequency and phase of the wave, respectively. A_1 and A_2 are wave magnitudes for the first image I_1 and the second image I_2 , while n_1 and n_2 are additive noise. u is the displacement between these two images at position (p, q) along the p direction.

The flow chart for the 3D algorithm is shown in Figure 2. After obtaining the Fourier transform of the input volumes $V_1(x, y, z)$ and $V_2(x, y, z)$ (temporal frames at time n and time $n+1$), identical 3D band-pass filters are applied to both volumes to isolate corresponding spectral peaks in order to

produce a pair of complex volumes in the Fourier domain. Let us refer to the two complex volumes in Fourier domain following band-pass filtering as $\mathcal{V}_{bf1}(\omega_x, \omega_y, \omega_z)$ and $\mathcal{V}_{bf2}(\omega_x, \omega_y, \omega_z)$. Applying a low frequency band-pass filter (LPF) and a high frequency band-pass filter (HPF) to both \mathcal{V}_{bf1} and \mathcal{V}_{bf2} followed by an inverse Fourier transform leads to four complex volumes $V_{bfLf1}(x, y, z)$, $V_{bfHf1}(x, y, z)$, $V_{bfLf2}(x, y, z)$, and $V_{bfHf2}(x, y, z)$. The reasoning behind application of a LPF and a HPF to \mathcal{V}_{bf1} and \mathcal{V}_{bf2} is to determine the local spatial frequency by power spectra. Subsequently a down-sampled map of displacement u is the local quotient of phase difference and local frequency at that position. This map is resampled to the initial size of the volume. Repeating the same algorithm on two long axis (LA) datasets yields 3D displacements.

The power spectra and cross power spectrum are given by:

$$\begin{aligned} P_{Lf}(x, y, z) &= |V_{bfLf1}|^2 + |V_{bfLf2}|^2 \\ P_{Hf}(x, y, z) &= |V_{bfHf1}|^2 + |V_{bfHf2}|^2 \end{aligned} \quad (2)$$

$$P_{cc}(x, y, z) = V_{bfLf1} \bar{V}_{bfLf2} + V_{bfHf1} \bar{V}_{bfHf2}$$

where \bar{V} is the complex conjugate of V .

The local frequency ω_x and local displacement u can then be estimated from:

$$\omega_x(x, y, z) = \omega_c \sqrt{\frac{P_{Hf}}{P_{Lf}}} \quad u(x, y, z) = \frac{\arg(P_{cc})}{\omega_x} \quad (3)$$

where ω_c is the band-pass center-frequency.

IV. RESULTS

In order to assess the accuracy of the tracking results, we simulated 3D CSPAMM data with the same spatial resolution and tagging frequency as with the real data. Four image sequences were generated. For the first sequence, a 2 pixel rigid translation in the y direction was prescribed. The second simulated sequence encoded a gradually changing motion in the x, y, z directions. The third simulated sequence encoded a 3D contraction. We also simulated a fourth sequence which represented a 3D expansion.

The 3D SinMod algorithm was applied to the two volumetric frames for each of the four simulated data: a reference undeformed volume and a deformed volume data set, permitting comparison between algorithm-estimated and the ground-truth deformations. In Table I, the tracking performance of the proposed 3D SinMod method is reported. Tracking error was calculated for every material points within the 3D volume. As can be seen in Table I, the technique produces highly accurate deformation fields with very small errors.

Five real 4D CSPAMM data sets from normal subjects were also used to validate the proposed 3D SinMod algorithm. For each data, there were 20 – 24 time frames \times 3

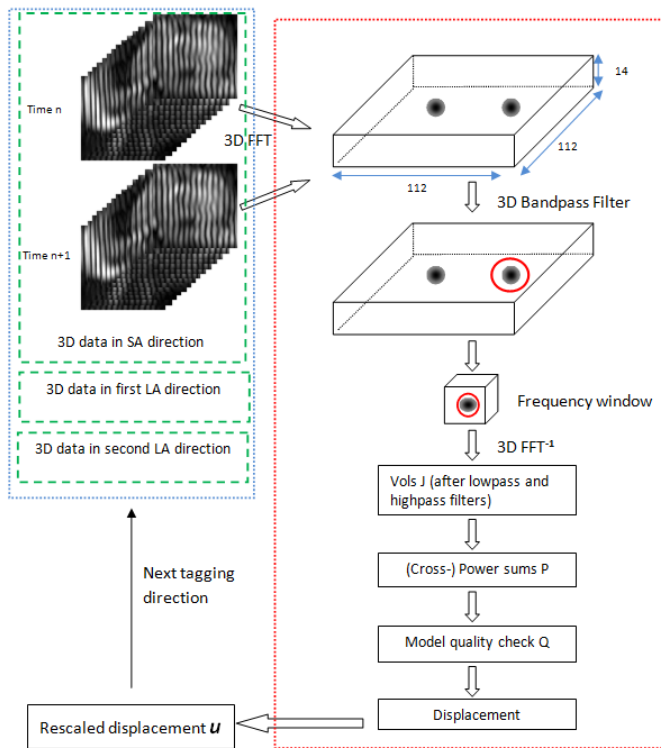


Fig. 2. Flow diagram of 3D SinMod algorithm for computing 3D displacements. Two stacks of 3D image volumes at time n and $n + 1$ are transformed to frequency domain via FFT. A 3D bandpass filter is applied to separate one off-center spectrum. Inverse FFT of a window around the band-passed frequencies results in down-sampled complex volume J . Further analysis yields a down-sampled map of displacement μ . This map is subsequently resampled to the initial size of the volume. Repeating the same algorithm for the two LA directions allows 3D displacement computation.

	AveError
Translation in Y	0.0043
Translation in X,Y,Z	0.0329
Contraction	0.0067
Expansion	0.0079

Table I. The average error between calculated motion fields and ground truth for simulated sequences with Gaussian noise added to the simulated data with standard deviation 0.05. The reported errors are in pixels.

image volumes, with 14 slices in each volume. Therefore, there were about $20 \times 3 \times 14 = 840$ images in each data set. All tag lines on 11 slices (from apex to base) and over 11 systolic phases for each of the three x , y , and z tagged volumes in five in-vivo 3D CSPAMM tagged data sets were manually delineated. Subsequently, the manually delineated tag lines at reference time were warped to all subsequent frames and the location of the warped tag lines were compared to location of manually delineated tag lines at time $t+1$ and an average error over for each phase (averaged over x , y , and z tagged volumes) was computed. Figure 3 displays the average error as a function of time for each of the 5 data sets.

V. CONCLUSION

In this paper, a novel 3D SinMod algorithm for analysis of 3D myocardial deformations has been proposed. In general in comparison to SPAMM tagged MRI, use of 3D CSPAMM is expected to yield accurate deformation fields throughout the cardiac cycle, owing to resolution of the tag fading issues encountered in SPAMM [11]. In order to quantitatively evaluate the accuracy of the methods, simulated data sets with known ground truth motion were used, showing sub-voxel precision. Results on five 4D in vivo CSPAMM data sets are very promising. The proposed framework permits accurate and automatic determination of both in-plane and out-of-plane components of motion of the left ventricular myocardium.

Acknowledgment

We would like to thank Professor Theo Arts for useful discussions about SinMod technique.

VI. REFERENCES

- [1] E. A. Zerhouni, D. M. Parish, W. J. Rogers, A. Yang, and E. P. Shapiro, "Human heart: Tagging with MR imaging—a method for noninvasive assessment of myocardial motion," *Radiology*, vol. 169, no. 1, pp. 59–63, October 1988.
- [2] L. Axel and L. Dougherty, "MR imaging of motion with spatial modulation of magnetization," *Radiology*, vol. 171, no. 3, pp. 841–845, June 1989.
- [3] T. Arts, F. W. Prinzen, T. Delhaas, J. Milles, A. Rossi, and P. Clarysse, "Mapping displacement and deformation of the heart with local sine wave modeling," *IEEE Transactions on Medical Imaging*, vol. 29, no. 5, pp. 1114–1123, May 2010.
- [4] N. F. Osman, W. S. Kerwin, E. R. McVeigh, and J. L. Prince, "Cardiac motion tracking using CINE harmonic phase (HARP) magnetic resonance imaging," *Magnetic Resonance in Medicine*, vol. 42, no. 6, pp. 1048–1060, December 1999.

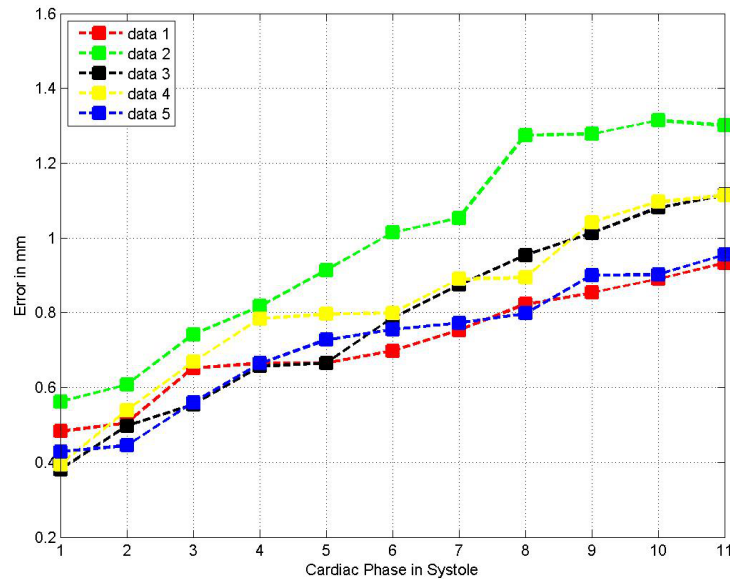


Fig. 3. 3D SinMod’s average error as a function of time for determining tag line displacements during systole for 5 in-vivo data sets. Results for data sets 1, 2, 3, 4, and 5 are differentiated with red, green, black, yellow, and blue colors. Please note that the error for each time point was calculated from the error between warped tag line locations and manually delineated tag lines on all image slices. Also, note that the manually delineated tag lines at the reference frame were warped to all subsequent frames and results were compared with the actual location of tag lines. This explains the reason for the increased error in later phases.

[5] H. Wang and A. A. Amini, “Accurate 2-D cardiac motion tracking using scattered data fitting incorporating phase information from MRI,” in *Proceedings of SPIE Medical Imaging 2010: Biomedical Applications in Molecular, Structural, and Functional Imaging*, February 2010, vol. 7626.

[6] H. Wang and A. A. Amini, “Cardiac motion tracking approach with multilevel B-splines and SinMod from tagged MRI,” in *Proceedings of SPIE Medical Imaging 2011: Biomedical Applications in Molecular, Structural, and Functional Imaging*, February 2011, vol. 7965.

[7] A. F. Frangi, W. J. Niessen, and M. A. Viergever, “Three-dimensional modeling for functional analysis of cardiac images: A review,” *IEEE Transactions on Medical Imaging*, vol. 20, no. 1, pp. 2–25, January 2001.

[8] H. Wang and A. A. Amini, “Cardiac motion and deformation recovery from MRI: A review,” *IEEE Transactions on Medical Imaging*, vol. 30, no. 2, pp. 487–503, February 2012.

[9] El-SH Ibrahim, “Myocardial tagging by cardiovascular magnetic resonance: evolution of techniques—pulse sequences, analysis algorithms, and applications,” *Journal of Cardiovascular Magnetic Resonance*, vol. 13, no. 36, July 2011.

[10] A. K. Rutz, S. Ryf, S. Plein, P. Boesiger, and S. Kozerke, “Accelerated whole-heart 3D CSPAMM for myocardial motion quantification,” *Magnetic Resonance in Medicine*, vol. 59, no. 4, pp. 755–763, April 2008.

[11] S. E. Fischer, G. C. McKinnon, S. E. Maier, and P. Boesiger, “Improved myocardial tagging contrast,” *Magnetic Resonance in Medicine*, vol. 30, no. 2, pp. 191–200, August 1993.